Electronic Supplementary Information for Energy & Environmental Science

Supporting Information

Highly Active Cobalt Phosphate and Borate Based Oxygen Evolving Catalysts Operating in Neutral and Natural Waters

Arthur J. Esswein,[a] Yogesh Surendranath,[b] Steven Y. Reece,[a] and Daniel G. Nocera[b]

[a] *Sun Catalytix Corporation, 200 Technology Square Suite 103 Cambridge, MA 02139,* [b] *Massachusetts Institute of Technology, 77 Massachusetts Avenue Cambridge, MA 02139*

nocera@mit.edu

Contents *Page*

Experimental Methods

Materials. $Co(NO_3)_2$ 99.999% (Aldrich or Strem) and KOH 85% (VWR) were used as received. Unless otherwise stated, electrolyte solutions were prepared with reagent grade water (Ricca Chemical, 18 MΩ-cm resistivity). Fluorine-tin-oxide coated glass (FTO, TEC-7) was purchased as pre-cut 1 cm × 2.5-3 cm glass pieces from Hartford Glass. Unless otherwise stated, all experiments used FTO with 7 Ω/sq surface resistivity.

Electrochemical Methods. All electrochemical experiments were conducted using a CH Instruments 730C or 760C potentiostat or a multichannel potentiostat from Arbin Instruments, a BASi Ag/AgCl or CH Instruments Hg/HgO reference electrode, and a high surface area Ni-foam or Pt-mesh counter electrode. All electrochemical experiments, except those utilizing a flow cell, were performed using a three-electrode cell with a porous glass frit separating the working and auxiliary compartments. Each compartment consisted of 50 mL of electrolyte solution. Unless otherwise stated, all experiments were performed at ambient temperature (21 ± 1 °C) and electrode potentials were converted to the NHE scale using E(NHE) = E(Ag/AgCl) + 0.197 V or E(NHE) = E(Hg/HgO) + 0.108 V.[1] Thermodynamic potentials for water splitting were calculated from standard potentials by correcting for solution pH using the relation $E = E^o - 0.059V(pH)$. An additional correction for the partial pressure of oxygen was also applied in computing the thermodynamic potential for experiments conducted at low current density using the Nernst equation. For experiments conducted at high current density, it was assumed that the solution proximal to the working electrode is saturated with oxygen and therefore no oxygen partial pressure correction is necessary. In this way, thermodynamic potentials for water oxidation vs. NHE were calculated as 0.810V (0.817 V high current) in KPi at pH 7.0, 0.680 V (0.687 V high current) in KBi at pH 9.2 and 0.420 V (0.428 V high current) in 1 M KOH, assuming a solution pH of 13.6. All overpotentials were computed using $\eta = E_{measured}(NHE) - E_{thermodynamic}(NHE)$.

Dependence of Anode Activity on Film Thickness. For this study, catalyst films were prepared via controlled-potential electrolysis of Bi electrolyte solutions containing 0.5 mM Co^{2+}. Depositions were carried out using an FTO-coated glass piece as the working electrode. FTO-coated glass pieces were rinsed with acetone and water prior to use in all experiments and a ~0.5 cm wide strip of Scotch tape was affixed to the FTO coated side such that a 1 cm^2 area was exposed to solution. Controlled potential electrolysis was carried out on quiescent solutions at 0.92 V with passage of 12, 24, 48, 96, 192 and 384 mC/cm^2 to produce films of varying catalyst loading and thickness.

Current-potential data were obtained for the films of varying thickness by conducting controlled potential electrolyses in Bi electrolyte at a variety of applied potentials. Prior to film preparation, the solution resistance was measured in the electrolysis bath to be used for Tafel data collection using the *i*R test function. The electrolysis solution was exchanged for Co^{2+}-containing Bi

1. R. A. Nickell, W. H. Zhu, R. U. Payne, D. R. Cahela, and B. J. Tatarchuk, *J. Power Sources,* 2006, **161**, 1217.

electrolyte and the film was prepared by controlled-potential electrolysis as described above. Following film preparation, the working electrode was rinsed in fresh Co-free Bi electrolyte and transferred, without drying, to the same electrolysis bath from which the solution resistance was measured. The electrode was allowed to equilibrate with the electrolysis solution for 5 min while being held at the open circuit potential. The solution was stirred and steady-state currents were then measured at applied potentials that descended from 1.17 V to 0.96 V proceeding in 10-30 mV steps. For currents greater than 10 μA/cm^2, a steady state was reached at a particular potential in less than 400 sec. For currents lower than 10 μA/cm^2, longer electrolysis times (as great as 20 min) were utilized to ensure that a steady state had been achieved. Tafel data were collected twice in succession with a 5 min pause between runs during which the electrode was held at open-circuit. Current values obtained between the two successive runs were reproducible to within 10% in all cases. The solution resistance measured prior to the data collection was used to correct the Tafel plots for ohmic potential losses. The first of the two successive runs for each film thickness is shown in Figure S1. Interpolation of these Tafel plots was used to determine the steady state activity at η = 400 mV for each film thickness (Figure 2).

To obtain a direct measure of the catalyst loading, Co-Bi/ITO electrodes were produced independently with passage of the same deposition charges as described above. Immediately following electrodeposition of the catalyst film, the electrodes were rinsed with reagent grade water and allowed to dry in air. These electrodes were then submerged in a known volume of 2% HNO_3 to dissolve the catalyst coating. To ensure quantitative dissolution of the catalyst films, all electrode were incubated in 2% HNO_3 overnight following repeated sonication. The concentration of dissolved Co-ion was determined by ICP-OES by correlating the intensity of the Co atomic emission lines at 228.616 and 238.892 nm for the sample to those of a series of standard solutions measured immediately prior to the sample.

The thickness of the films was estimated by assuming that each cobalt is ligated by six oxygen atoms in an octahedral configuration. Assuming a Co–O distance of ~1.9 Å (as indicated by EXAFS data),[2,3] the primary coordination sphere of each cobalt atom occupies a cube 3.8 Å in width. Taking note of the high phosphate content of these films, it is more reasonable to assume, as an upper limit, that each Co occupies a cube 5 Å in width, defining a volume of 125 Å^3. This estimate is in line with EXAFS data of thin films that points to an average ordered structural unit consisting of 7 cobalt atoms arranged in a planar cobaltate lattice. This structural unit, taken together with several phosphates, defines a ~700 Å^3 slab. Thus, 125 Å^3/Co serves as a reasonable upper limit. Using this estimate, a film monolayer requires a loading of 3.4 nmol Co/cm^2 and is 0.5 nm thick. As such, the thinnest film, containing 0.11 μmol Co/cm^2, and the thickest film, containing 2.6 μmol Co/cm^2, are estimated to be 16 and 380 nm thick, respectively.

2. M. Risch, V. Khare, I. Zaharieva, L. Gerencser, P. Chernev, and H. Dau, *J. Am. Chem. Soc.*, 2009, **131**, 6936.

3. M. W. Kanan, J. Yano, Y. Surendranath, M. Dinča, V. K. Yachandra, and D. G. Nocera, *J. Am. Chem. Soc.*, 2010, **132**, ASAP, DOI: 10.1021/ja1023767.

The turnover frequency (TOF) of Co-Bi is determined from the slope of the activity loading plot (Figure 2) as described in the text. For Co_3O_4 nanorods,[4] a turnover frequency for O_2 evolution of 1140 s^{-1} per cluster under photochemical conditions was reported. To normalize this turnover frequency per cobalt atom in each cluster, the reported average dimensions for each nanorod, taken together with the average number of rods per cluster and the density of the Co_3O_4, was used to estimate that ~1.5×10^6 Co atoms (volume of a cylinder was used for a rod) comprised each nanocluster. Dividing the reported turnover frequency by this value yields a lower limit per cobalt of ~8×10^{-4} s^{-1}.

Enhancement of Anode Activity on High Surface Area Ni-Foam Electrodes. Catalyst films were prepared on high surface area Ni foam electrodes as described in the text. High surface Ni foam supports were degreased prior to electrodeposition by sonication for 5 min in an aqueous solution of Triton-X, followed by rinsing with distilled water and isopropyl alcohol. After cleaning, the foam samples were masked to expose 1 cm^2 of geometric electrode area using a robust and electrochemically insulating silicone adhesive. Deposition of the Co-OEC catalyst on the exposed active area was performed using 10 mM $Co(NO_3)_2 \cdot 6H_2O$ solutions in 0.1 M MePi buffer (pH 8.5) and applying a bias of 1.1 V vs. Ag/AgCl to the electrode. MePi buffer was chosen as the electrolyte (in place of KPi) owing to the greater solubility of Co^{2+} ions in this medium. The depositions proceeded using ~ 150 mL of solution in a single compartment cell with vigorous stirring to mitigate Co^{2+} mass transport limitations within the Ni foam. Catalyst deposition was rapid when using this procedure and the electrode quickly formed a thick black catalyst layer (Figure S3).

Steady state and sweeping polarization data for Co-OEC/Ni foam electrodes were collected using a custom-built, transparent polycarbonate flow-through electrochemical cell. The cell incorporates side ports for electrolyte flow and an angled top port designed to fit a BAS Ag/AgCl reference electrode and troughs cut for silicon o-ring seals, Figure S2. In a typical experiment two chambers were employed with the porous Co-OEC/Ni foam electrode sandwiched in between. Electrical connection to the Co-OEC/Ni foam anode was afforded by direct connection to an unmasked portion of the electrode protruding from cell hardware. Electrolyte leaking through the porous Ni foam was prevented by filling the non-active area with the inert silicone sealant. A coiled Pt wire was used as the auxiliary electrode. Electrical connection to the counter electrode was achieved by passing the Pt wire through a rubber stopper inserted in the top port on the upper chamber. The Ag/AgCl reference electrode was positioned behind the Co-OEC/Ni foam working electrode in the lower chamber (outside of the working/auxiliary electrode current path) to minimize ohmic potential losses (Figure S4). The flowing electrolyte was introduced into the bottom portion of the cell, was then forced through the 1 cm^2 active area of the porous Ni foam anode, before exiting the cell through a port on the upper section. In this configuration

4. F. Jiao and H. Frei, *Angew. Chem. Int. Ed.*, 2009, **48**, 1841.

the electrolyte aids in the removal of gas bubbles in the pores of the foam, which can limit electrode performance.

Sweeping polarization experiments from η = 100 to 640 mV were conducted at a slow scan rate of 1 mV/s to decrease to reduce the effects of electrode double layer charging on the observed current. Steady state experiments were conducted in galvanostatic mode, wherein the Co-OEC/ Ni foam anode was operated at a fixed current density of 100 mA/cm^2 and the overpotential monitored as a function of time. No iR correction was made to the observed potentials in the flow through experiments due to the positioning of the Ag/AgCl reference electrode outside of the working electrode/counter electrode current path.

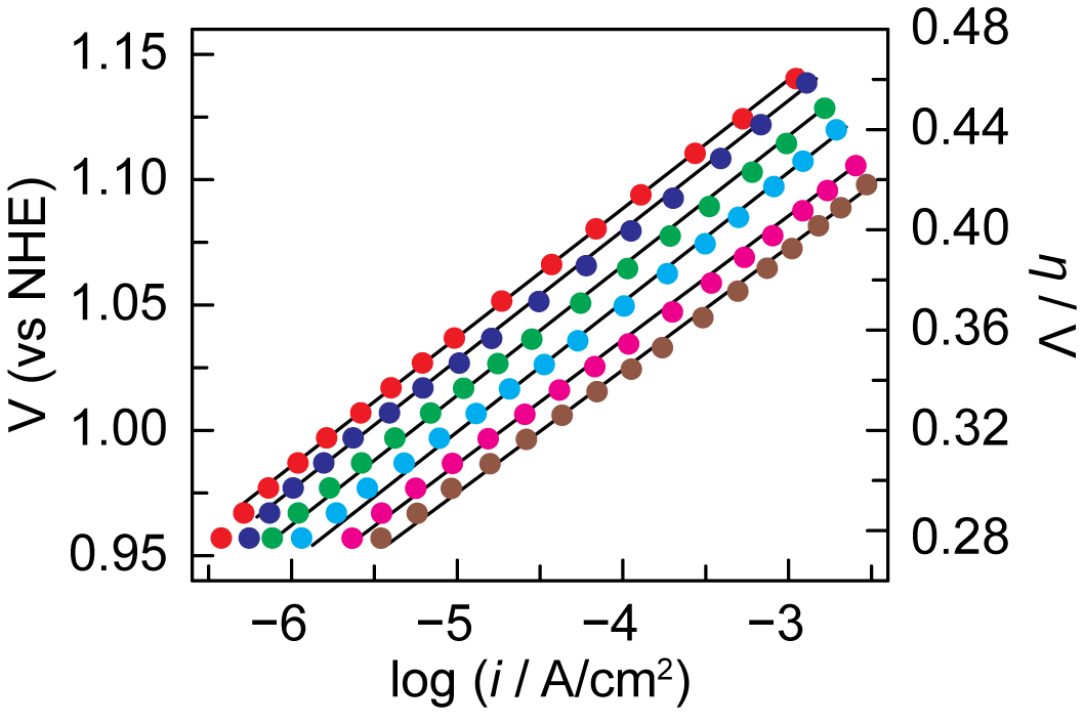

Figure S1. Tafel plots, V = (V_{appl} – iR), η = (V – E°), of catalyst films operated in cobalt-free 1 M Bi electrolyte, pH 9.2. Progressing from left to right, data correspond to 12, 24, 48, 96, 192, and 384 mC/cm^2 of deposition charge.

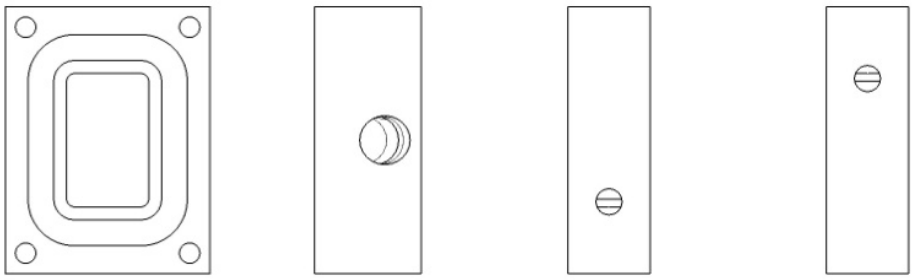

Figure S2. Front, Top, and side views of the electrochemical flow-cell showing the O-ring seal cutout, angled reference electrode port, and electrolyte flow ports, respectively.

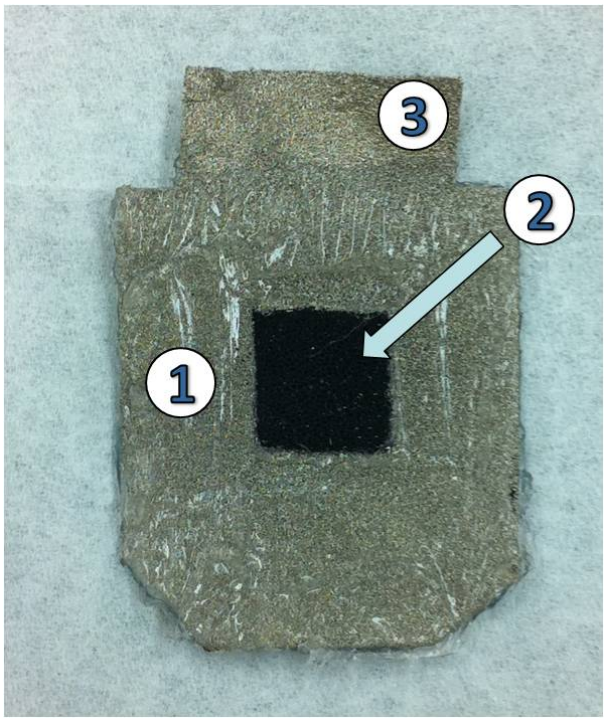

Figure S3. Typical Co-OEC/Ni Foam anode prepared as described in the text. Numbered items point attention to 1) area masked by silicone sealant, 2) active area of the porous Co-OEC/Ni foam working electrode, 3) unmasked portion of Ni foam that provides electrical contact outside of the flow through cell.

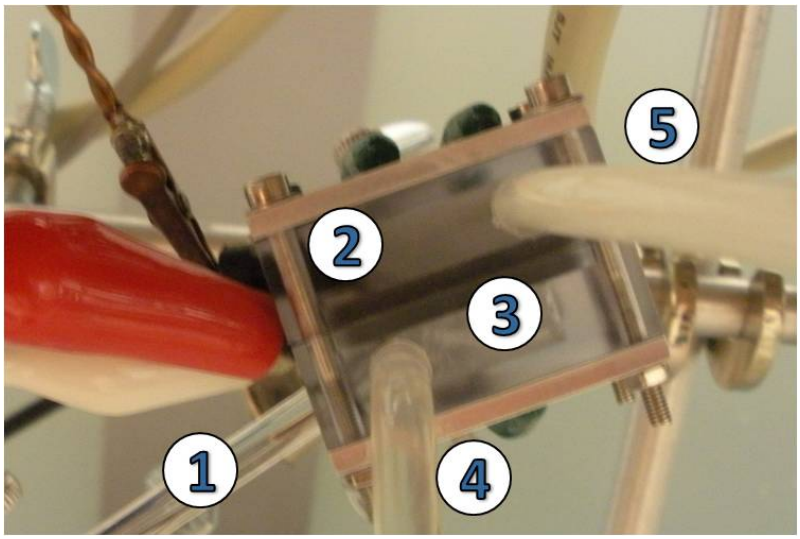

Figure S4. Typical configuration used for three electrode measurements on porous Co-OEC/Ni Foam anodes. Numbered items point attention to (1) Ag/AgCl reference electrode, (2) coiled Pt counter electrode, (3) porous Co-OEC/Ni foam working electrode, (4) electrolyte inlet, and (5) electrolyte outlet with the product gases. The aluminum endplates are employed to enforce uniform compression and reduce stress on the polycarbonate chamber parts.

Table S1. Tafel slope values for anodized Ni and Co-Bi/ITO anodes in 1.0 M KOH and 1.0 M KBi (pH 9.2) solutions

Electrode	**Water Supply**	**Tafel Slope (initial)** (mV/ decade current density)	**Tafel Slope (final)** [a] (mV/ decade current density)
Anodized Ni (1.0 M KOH)	18 MΩ-cm	35	36
	Charles River	103	154
	Seawater	116	129
Co-Bi/ITO (1.0 M KBi)	18 MΩ-cm	50	53
	Charles River	54	61
	Seawater	82	89

[a] after a 4 h electrolysis at 1 mA/cm^2

Table S2. Analysis of the Charles River and seawater samples used for the anode activity measurements.

Analyte	**Charles River Water**	
	Concentration (mg/L)	Concentration (mM)
Calcium	19	0.470
Magnesium	5.3	0.220
Potassium	3.6	0.092
Sodium	78	3.400
Iron	2.2	0.039
Analyte	**Seawater**	
	Concentration (mg/L)	Concentration (mM)
Calcium	340	8.5
Magnesium	1000	40
Potassium	420	11
Sodium	9600	42
Iron	<0.5	<0.009